

Supplemental Methods:

Mouse Tissue Preparation. Mice were anesthetized, euthanized, and immediately perfused with PBS from the left ventricle until blood was cleared. Kidneys were then removed, hemi-sectioned, and portions were snap frozen in liquid nitrogen or fixed with methacarn and paraffin-embedded or fixed with 4% paraformaldehyde. For frozen sections, fixed samples were subsequently immersed in 30% (w/v) sucrose, then embedded in optimum cutting temperature compound (OCT, Sakura FineTek) and 7- μ m sections were cut.

Mouse Tissue Histological Analysis. Histological analysis was performed on paraffin-embedded and serially cut kidney sections (3 μ m) stained with PAS, and Masson's trichrome. Histological changes associated with tubular injury were quantitated by calculation of the percent of tubules that displayed one or more of the following: cell necrosis, loss of brush border, cast formation, and tubule dilatation. Quantitation was as follows: 0, none; 1, \leq 10%; 2, 11–25%; 3, 26–45%; 4, 46–75%; and 5, $>$ 76% of tubules. This analysis was performed by an individual blinded to the genetics of the animals (2). The percentage of Masson's trichrome-positive area was determined with ImageJ software (<http://rsbweb.nih.gov/ezp-prod1.hul.harvard.edu/ij>). For these morphologic quantifications, 5 random visual fields (x200) were analyzed per kidney section.

RNA Extraction and Real-Time Quantitative PCR (qPCR). Total RNA was isolated from snap-frozen kidneys using the TRIzol reagent (Sigma) according to the standard protocol. First-strand cDNA was synthesized using the MML-V reverse transcriptase (Promega,

USA). qPCR was performed using the iQ-SYBR Green supermix (BioRad) and the iQ5 Multicolor Real-Time PCR Detection System (BioRad) for mRNA detection. 18S rRNA was used as housekeeping gene.

The following primer sequences were used:

18SrRNA forward: ATGGCCGTTCTTAGTTGGTG, reverse
GAACGCCACTTGTCCCTCTA;

Atr forward: ACTCTGGCTGTAGCGTCCTTTC; reverse:
TGCTTCTTTTCTGTAATAAATGACTCAAA;

KIM-1 forward: AAACCAGAGATTCCCACACG,
reverse: GTCGTGGGTCTTCCTGTAGC;

TNF- α forward: CCCTGAGGGGGCTGAGCTCAA,
reverse ACCTGCCCGGACTCCGCAA;

IL-1 β forward: CCTTCCAGGATGAGGACATGA,
reverse: AACGTCACACACCAGCAGGTT;

TGF- β forward: GCAACAATTCCTGGCGTTACC,
reverse: CGAAAGCCCTGTATTCCGTCT;

CTGF forward: AACAGTGGAGATGCCAGGAG,
reverse TAATTTCCCTCCCCGGTTAC;

Col1 α 1 forward: TGACTIONGGAAGAGCGGAGAGT,
reverse: GTTCGGGCTGATGTACCAGT;

fibronectin forward: ATGTGGACCCCTCCTGATAGT,
reverse: GCCCAGTGATTCAGCAAAGG.

α SMA forward: AGGGCTGGAGAATTGGATCT,

reverse: CCAGCAAAGGTCAGAGAAGG;

PDGFR- β forward: CACCTTCTCCAGTGTGCTGA,

reverse: GTGGGATCTGGCACAAAGAT;

p53 forward: CACAGCGTGGTGGTACCTTA, reverse: TCTTCTGTACGGCGGTCTCT;

p21 forward: GTGGGTCTGACTCCAGCCC, reverse: CCTTCTCGTGAGACGCTTAC

Primary culture of mouse renal tubular epithelial cells. Primary cultures of mouse renal tubular epithelial cells from both ATR^{RPTC^{-/-}} and ATR^{Ctrl} mouse kidneys were made using established protocols (3). Briefly, both ATR^{RPTC^{-/-}} and ATR^{Ctrl} mice (22 weeks) were administered intraperitoneally 3 doses of tamoxifen (3 mg, Sigma-Aldrich), dissolved in 3% (vol/vol) ethanol-containing corn oil (Sigma-Aldrich), every other day. 9 weeks later, mice were sacrificed and the kidney cortex was dissected, minced and then digested in medium containing collagenase (10 μ g/ml) for 40 minutes at 37°C. The enzyme reaction was terminated by FBS. Glomeruli and remaining tissue clumps were separated by decanting after 1 minute of gravity sedimentation. After washing 2 times in medium, tubules were resuspended in tubule medium (DMEM/F-12 with transferrin, insulin, selenium, hydrocortisone, EGF, and BSA). They are then aliquoted into 10 cm dishes coated with BD Matrigel Matrix Phenol Red-Free (BD Biosciences 356237). The epithelial cells were used in experiments on day 7 of culture.

Cell cycle analysis with DNA content dye. On day 0, each 3.0×10^5 mouse primary epithelial cells (ATR^{RPTC^{-/-}} and ATR^{Ctrl}) were seeded on 12-well plates. On day 3, media were replaced to DMEM with or without 0.2 μ g/ml cisplatin. After 24 hours exposure to

cisplatin, cells are detached with 0.25% Trypsin/0.1% EDTA, fixed with 2% paraformaldehyde/5% FBS in PBS, and then stained with FxCycle Violet Stain (Invitrogen F10347). Cells were analyzed by FACS Canto II (BD Biosciences). Data were analyzed using FLOWJO (FLOWJO).

Immunofluorescence Analysis and Antibodies. Cryosections of 7 μ m were mounted on Fisher Superfrost Plus (Fisher) microscope slides, air dried, and treated for immunofluorescence as described (4). Primary antibodies against the following proteins were used: kidney injury molecule-1 (KIM-1) (goat, 1:500 AF1817; R&D Systems); F4/80 (1:100, HB-198; ATCC Hybridoma) (5); kidney specific protein (KSP) (mouse biotin coupled, 1:100, kindly provided by Hiroshi Itoh and Toshiaki Monkawa (Keio University School of Medicine) (6)); SMA (mouse Cy3 coupled, 1:500, cat. no. F3777, Sigma-Aldrich); Ki67 (rabbit monoclonal, 1:1000, cat. no. VP-RM04; Vector Laboratories); phosphorylated H2AX (Ser139) (γ H2AX) (rabbit monoclonal, 1:100 cat. no. #9718; Cell Signaling); cleaved caspase-3 (Asp175) (rabbit, 1:100, cat. no. #9661; Cell Signaling) ; phospho-Histone H3 (Ser10) (rabbit, 1:100, cat. no. 06-570; EMD Millipore) ; mTOR (Cell Signaling Technology, 7C10, rabbit, 1:50); LC3 (Nanotools, mouse, 5F10, 1:50). Secondary antibodies were either FITC-, Cy3-, or Cy5- conjugated (Jackson ImmunoResearch). Nuclear counterstaining was performed using DAPI and followed by mounting in Prolong-Gold (Invitrogen). Images were obtained by confocal (Nikon C1 Eclipse; Nikon) microscopy. For all morphological quantifications, 5 random (x200) or 10 random (x400) visual fields were analyzed per kidney section, and percentage of KIM-1, KSP and F4/80-positive area, or number of γ H2AX, cleaved caspase-3, Ki67 and pH3-

positive cells were determined with ImageJ software (7). All images were obtained by standard or confocal microscopy (Eclipse 90i, C1 Eclipse, respectively; both from Nikon).

Senescence-associated β -galactosidase (SA- β -gal) staining. SA- β -gal staining in mouse kidney tissues was performed using a Senescence β -Galactosidase Staining Kit (#9860; Cell Signaling), following the manufacturer's instructions. For quantification, 5 random (x200) visual fields were analyzed per kidney section, and percentage of SA- β -gal+ area of the section was determined with ImageJ software (7).

Western blot analysis. Kidney tissues were lysed in RIPA buffer (50 mmol/l Tris/HCl, 1% NP-40, 0.25% deoxycholic acid, 150 mmol/l NaCl, 1 mmol/l EGTA, 1 mmol/l sodium orthovanadate, and 1 mmol/l sodium fluoride) with protease inhibitor (Sigma-Aldrich) and quantified by Bradford protein assay. Membranes were incubated with the following primary antibodies: anti-KIM-1 (goat, 1:500 AF1817; R&D Systems); ATR (1:500, sc-1887; Santa Cruz Biotechnology) ; p53 (1:1000, sc-126; Santa Cruz Biotechnology) ; p21 (1:1000, sc-6246; Santa Cruz Biotechnology) ; β -actin (1:1000, #4967; Cell Signaling) ; CTGF-specific antibody (GeneTex 1:1,000). Horseradish peroxidase-conjugated secondary antibodies were applied, and enhanced chemiluminescence (Amersham Biosciences) was used to detect proteins. The ECL film was scanned using a commercial office scanner (Epson Expression 1680 Scanner) and evaluated in ImageJ.

Cell Culture and Treatment. Human HKC-8 proximal tubular epithelial cell lines were kindly provided by L. Racusen (Baltimore, MD, USA) (8). LLC-PK1 cells were purchased

from ATCC. The mRPTC cell line was kindly provided by R Zent (Nashville, TN, USA). The MTT (3-(4,5-dimethylthiazol-2-yl)-2,5-diphenyltetrazolium bromide) tetrazolium reduction assay was used for evaluation of viability (9). Cells were seeded into a 96 well plate (0.1×10^4 cells/well) and allowed to grow overnight. Serum-starved HKC-8 cells were incubated with 10 μ M of ATR inhibitor; VE-821 (10, 11) (Axon Medchem, Reston, VA) 2 hours before treatment. Then cells were cultured in 21 % or 5 % O₂ with or without 30 μ g/ml of cisplatin for 24 hours.

References

1. Matsuo S, Imai E, Horio M, Yasuda Y, Tomita K, Nitta K, et al. Revised equations for estimated GFR from serum creatinine in Japan. *American journal of kidney diseases : the official journal of the National Kidney Foundation*. 2009;53(6):982-92.
2. Melnikov VY, Faubel S, Siegmund B, Lucia MS, Ljubanovic D, and Edelstein CL. Neutrophil-independent mechanisms of caspase-1- and IL-18-mediated ischemic acute tubular necrosis in mice. *J Clin Invest*. 2002;110(8):1083-91.
3. Ichimura T, Asselton EJ, Humphreys BD, Gunaratnam L, Duffield JS, and Bonventre JV. Kidney injury molecule-1 is a phosphatidylserine receptor that confers a phagocytic phenotype on epithelial cells. *The Journal of clinical investigation*. 2008;118(5):1657-68.
4. Ichimura T, Bonventre JV, Bailly V, Wei H, Hession CA, Cate RL, et al. Kidney injury molecule-1 (KIM-1), a putative epithelial cell adhesion molecule containing a novel immunoglobulin domain, is up-regulated in renal cells after injury. *J Biol Chem*. 1998;273(7):4135-42.
5. Ichimura T, Hung CC, Yang SA, Stevens JL, and Bonventre JV. Kidney injury molecule-1: a tissue and urinary biomarker for nephrotoxicant-induced renal injury. *Am J Physiol Renal Physiol*. 2004;286(3):F552-63.
6. Morizane R, Fujii S, Monkawa T, Hiratsuka K, Yamaguchi S, Homma K, et al. miR-34c attenuates epithelial-mesenchymal transition and kidney fibrosis with ureteral obstruction. *Scientific reports*. 2014;4:4578.
7. Grgic I, Campanholle G, Bijol V, Wang C, Sabbisetti VS, Ichimura T, et al. Targeted proximal tubule injury triggers interstitial fibrosis and glomerulosclerosis. *Kidney international*. 2012;82(2):172-83.
8. Racusen LC, Monteil C, Sgrignoli A, Lucskay M, Marouillat S, Rhim JG, et al. Cell lines with extended in vitro growth potential from human renal proximal tubule: characterization, response to inducers, and comparison with established cell lines. *The Journal of laboratory and clinical medicine*. 1997;129(3):318-29.

9. Alley MC, Scudiero DA, Monks A, Hursey ML, Czerwinski MJ, Fine DL, et al. Feasibility of drug screening with panels of human tumor cell lines using a microculture tetrazolium assay. *Cancer research*. 1988;48(3):589-601.
10. Reaper PM, Griffiths MR, Long JM, Charrier JD, McCormick S, Charlton PA, et al. Selective killing of ATM- or p53-deficient cancer cells through inhibition of ATR. *Nature chemical biology*. 2011;7(7):428-30.
11. Mateos-Gomez PA, Gong F, Nair N, Miller KM, Lazzerini-Denchi E, and Sfeir A. Mammalian polymerase theta promotes alternative NHEJ and suppresses recombination. *Nature*. 2015;518(7538):254-7.

Supplemental Table 1 Clinical parameters of CKD and MCD patients.

| MCD | Age | Sex | Clinical diagnosis at kidney biopsy | DM | HTN | Creatinine (mg/dl) | eGFR (ml/min/1.73m ²) | U-protein (g/gCre) | Pathological diagnosis | Fibrosis |
|------------|-----|-----|--|----|-----|--------------------|-----------------------------------|--------------------|---|----------|
| 1 | 57 | M | Nephrotic syndrome | - | - | 0.9 | 68 | 6.9 | Minimal change | 0 |
| 2 | 47 | M | Nephrotic syndrome | - | - | 1.04 | 62 | 13.62 | Minimal change | 1 |
| 3 | 63 | F | Nephrotic syndrome | - | - | 0.62 | 73 | 8.32 | Minimal change | 1 |
| 4 | 64 | F | Nephrotic syndrome | - | - | 0.68 | 66 | 12.4 | Minimal change | 1 |
| 5 | 37 | F | Nephrotic syndrome | - | - | 0.63 | 84 | 9.64 | Minimal change | 0 |
| 6 | 17 | M | Asymptomatic Proteinuria and Hematuria | - | - | 0.71 | 112 | 0.3 | Minimal change | 0 |
| 7 | 22 | M | Asymptomatic Proteinuria | - | - | 0.7 | 118 | 0.47 | Minimal change | 0 |
| 8 | 34 | M | Asymptomatic Proteinuria and Hematuria | - | - | 0.78 | 93 | 0.01 | Minimal change | 0 |
| 9 | 59 | M | Asymptomatic Proteinuria and Hematuria | - | + | 0.96 | 68 | 0.13 | Minimal change | 1 |
| CKD | | | | | | | | | | |
| 1 | 78 | M | Chronic renal failure/Nephrotic syndrome | + | + | 4.44 | 19 | 12.78 | Diabetic nephropathy and Membranous nephropathy | 2 |
| 2 | 59 | M | Chronic renal failure | + | + | 1.93 | 42 | 3.09 | Nephrosclerosis | 3 |
| 3 | 66 | M | Chronic renal failure/Nephrotic syndrome | + | + | 2.73 | 11 | 7.49 | Diabetic nephropathy | 4 |
| 4 | 66 | M | Chronic renal failure/Nephrotic syndrome | + | + | 1.36 | 28 | 5.94 | Diabetic nephropathy | 3 |
| 5 | 73 | M | Chronic renal failure/Nephrotic syndrome | + | + | 3.84 | 13 | 14.5 | Diabetic nephropathy with severe fibrosis | 3 |
| 6 | 51 | F | Chronic glomerulonephritis | - | - | 0.91 | 51 | 6.13 | Mesangial proliferative glomerulonephritis with severe fibrosis | 4 |
| 7 | 57 | M | Chronic glomerulonephritis | + | + | 1.05 | 58 | 0.78 | Mesangial proliferative glomerulonephritis | 2 |
| 8 | 77 | M | Chronic renal failure | + | + | 2.49 | 21 | 4.74 | Nephrosclerosis | 4 |
| 9 | 22 | M | Chronic renal failure | - | - | 1.4 | 54 | 1.09 | Mesangial proliferative glomerulonephritis with severe fibrosis | 4 |
| 10 | 41 | F | Chronic renal failure | - | + | 1.81 | 26 | 1.45 | Mesangial proliferative glomerulonephritis with severe fibrosis | 4 |
| 11 | 45 | M | Chronic renal failure | - | - | 1.53 | 41 | 2.83 | Focal segmental glomerulosclerosis | 4 |

CKD: chronic kidney disease

MCD: minimal change disease

estimated GFR (mL/min/1.73 m²) = 194 × Cr^{-1.094} × Age^{-0.28} (in case of female ×0.739) (76)

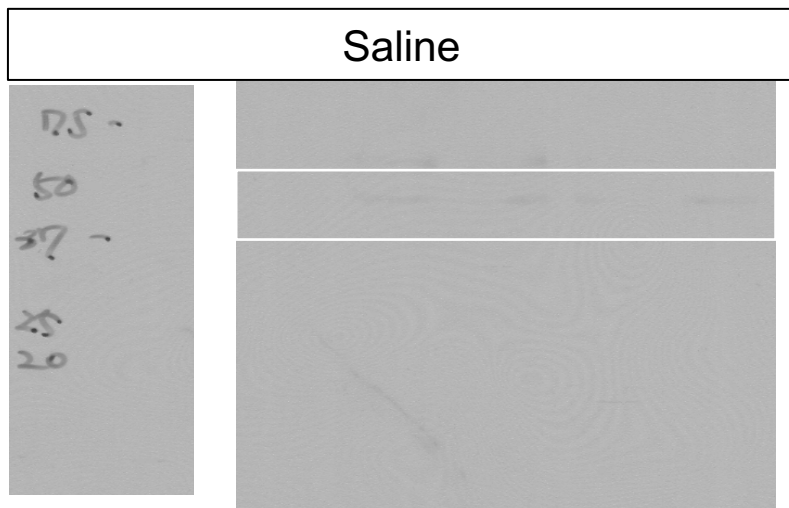
76. Matsuo S, Imai E, Horio M, Yasuda Y, Tomita K, Nitta K, et al. Revised equations for estimated GFR from serum creatinine in Japan. American journal of kidney diseases : the official journal of the National Kidney Foundation. 2009;53(6):982-92.

Supplemental Movie Legend:

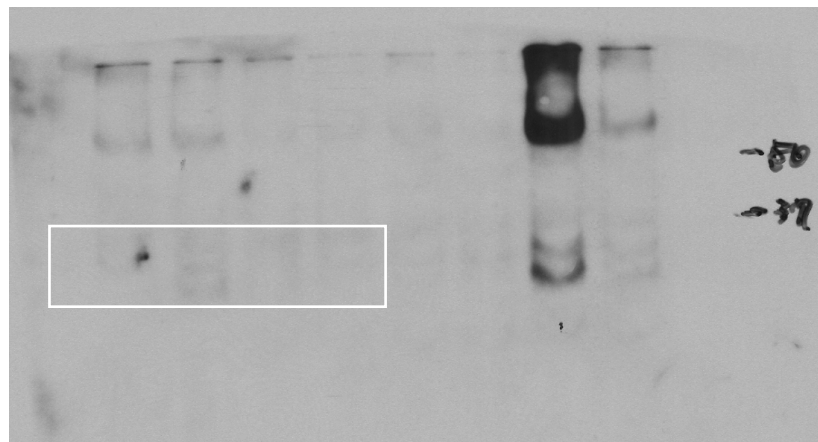
Supplemental Movie. TASCSC structures in ATR depleted tubules. Kidneys from ATR^{RPTC-}_{/-} mice were stained for mTOR (red), LC3 (green) and DNA (DAPI, blue) and imaged by SIM. The resulting micrographs were rendered as 3D surfaces using Imaris software. The video displays the 3D surfaces for all channels showing the overall tubule structure, with the lumen in the middle, and zooms in on two highly connected structures, one positive for mTOR and the other for LC3, which is the definition of a TASCSC. Note: Surfaces are rendered as solid objects and do not display overlap by mixing the channels, i.e. green/red overlap does not display as yellow.

Unedited gel for Figure 3 - E

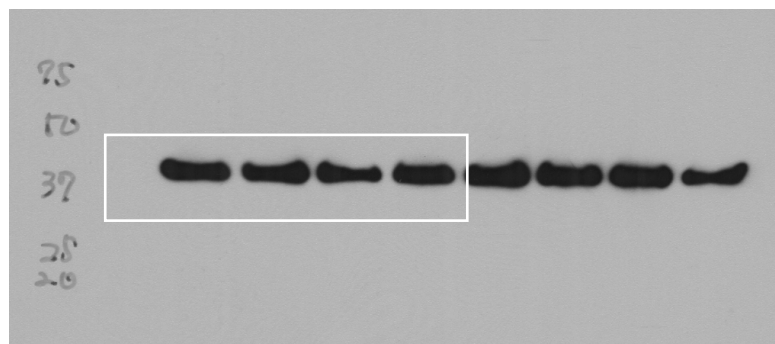
p53



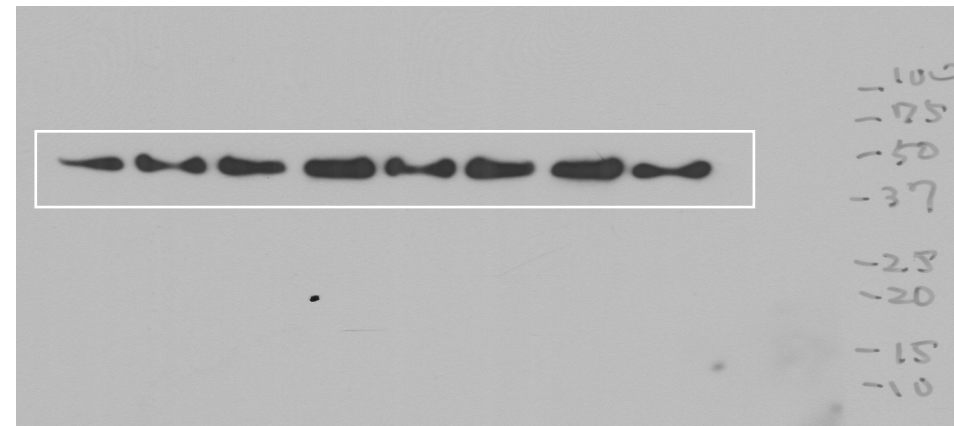
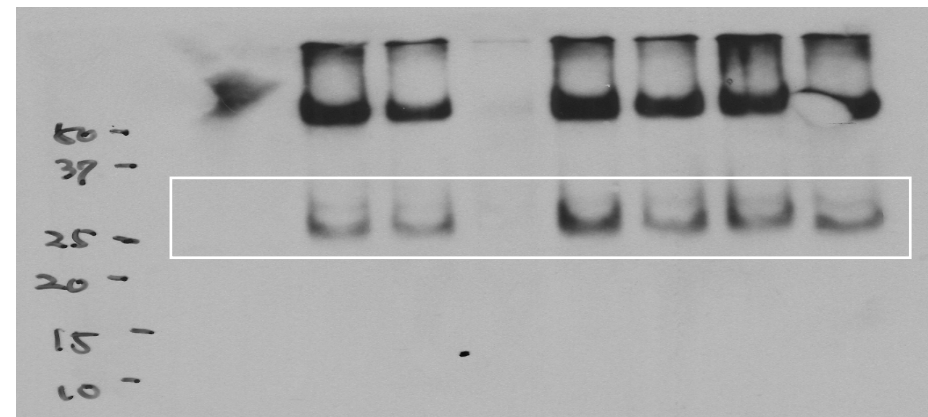
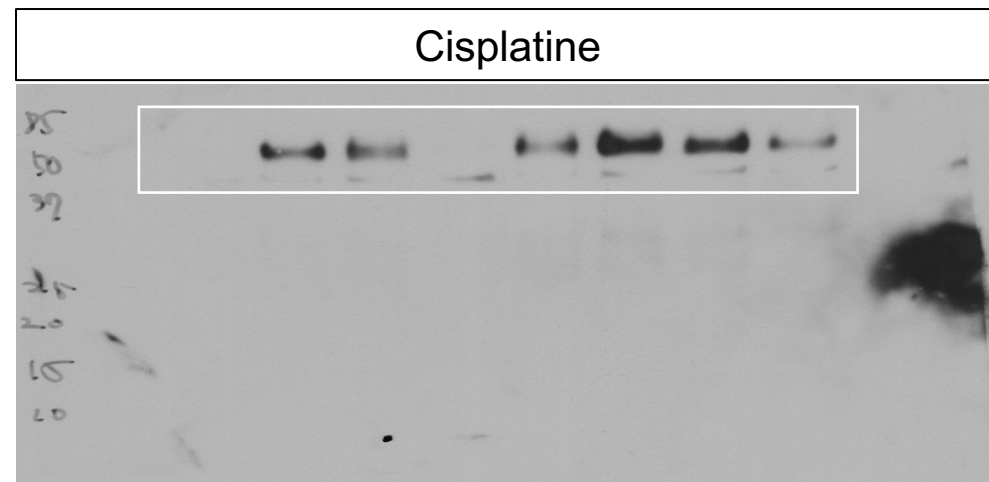
p21



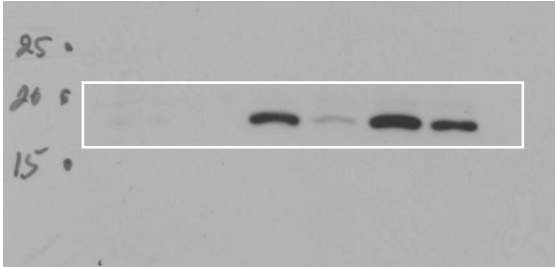
β actin



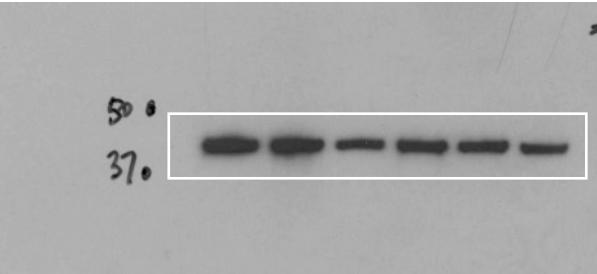
Cisplatin



Unedited gel for Figure 3 - I

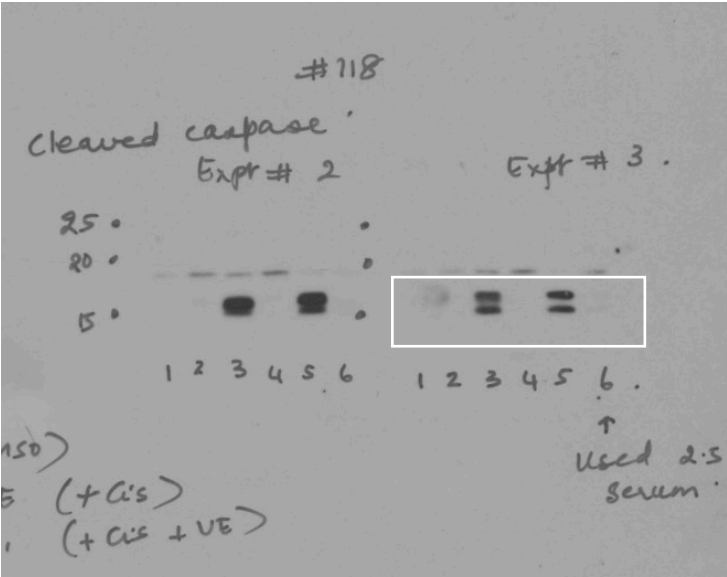


Cleaved caspase-3

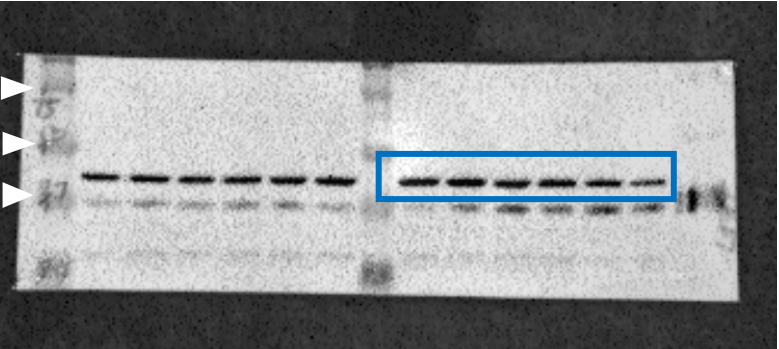


β Actin

Unedited gel for Figure 3 - J



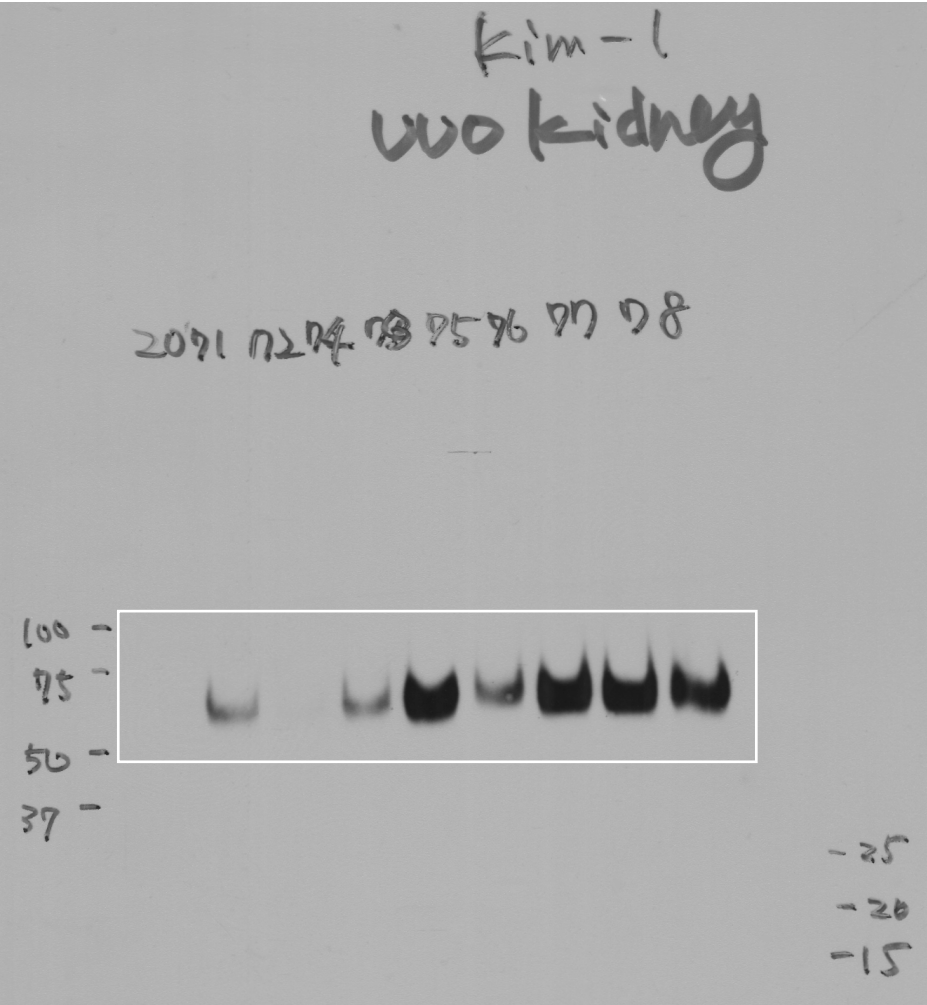
Cleaved caspase-3



β Actin

Unedited gel for Figure 5 - C

KIM-1



β actin

